STRUCTURAL MONITORING OF FILAMENTARY COMPOSITES USING EMBEDDED FIBER OPTICS

by

John L. Cashon, David L. Lehner, Mark V. Bower, John A. Gilbert*
University of Alabama in Huntsville, Huntsville, Alabama

Abstract

Sensors, such as electrical resistance strain gages, have been used for decades to make measurements on the outside surfaces of structural components. This approach to testing was adequate, since most of the structures in question were fabricated using homogeneous materials where stresses maximize on the free surface. However, many components of advanced structures for space based applications, such as those proposed for Space Station, incorporate filamentary composite materials. The inhomogeneous nature of these materials coupled with imperfections created during their fabrication or service may lead to stress concentrations within the composite matrix itself. These factors necessitate the ability to continuously monitor overall structural integrity and call for a modified approach to experimental testing.

This paper explores the potential of monitoring overall structural integrity by embedding monomode optical fibers between lamina of a composite beam constructed of kevlar29/epoxy cloth. Phase changes are monitored in three different fibers as the beam is subjected to pure bending. The embedded fibers, aligned with the longitudinal axis of the beam, are located just below the top surface, in a plane between the mid-plane and the top surface, and at the mid-plane. The strain response of the optical fibers is compared to strain gage readings taken at the surface. Results show a strong correlation between phase and applied deformation.

1. Introduction

"Smart skin" technology relies on the fact that avionics, actuators, and structural sensors can be integrated with, or embedded within, layers of structural fibers in a composite matrix. In this futuristic scenario, avionics such as antennas, digital processors, and "black boxes" will serve as structural members; embedded actuators, including shape memory alloys, electrorheological fluids, and piezoelectric materials will aid in advancing flight control surfaces; and, embedded sensors will measure delaminations, vibrations, impact damage, cracks, strain, and fatigue in structural components. The smart skin approach to aircraft design is attractive, since it can be used to reduce weight, to increase interior space or reduce overall size, and to provide real time analysis of structural integrity.[1] These attributes allow design engineers to better utilize the performance envelope, optimize scheduling of required structural checks, and reduce the risk of in-flight mishaps.

Several authors have discussed various aspects for the successful development of a cost effective smart skin system, and most agree that embedded optical fibers provide great potential for realizing this goal.[2-4] Some of the physical properties that make glass fibers attractive for use in a smart skin system are: (1) they expand and contract in the presence of acoustic waves, (2) they are light weight and dimensionally small, (3) they can withstand high and low temperature extremes, (4) they expand or contract due to temperature variations, (5) their optical properties change when strained, (6) they are easily embedded between layers of composite materials, (7) they behave as insulators electrically, (8) they facilitate remote sensing, and (9) are excellent communication lines.

Optical fibers could be embedded into filamentary composites in the manufacturing stage to monitor the curing process for optimal cure and for the accurate determination of residual stresses or strains. The same system would allow non-destructive testing of the component prior to installation on an aerospace vehicle or system and could be used to verify the results obtained by other diagnostic methods such as holographic interferometry, speckle metrology, and ultrasonic testing. As parts are integrated, optical fibers could be connected to a fiber optic nervous system for health monitoring. The fiber optic nervous system could be made redundant or reconfigurable so that critical areas could be accessed should one or more fibers be damaged.

Ironically, widespread incorporation of composites into new aerospace vehicles has

---

* J. Cashon and D. Lehner are Graduate Research Assistants, M. Bower is Assistant Professor, and J. Gilbert is Professor in the Department of Mechanical Engineering. Dr. Bower is an Associate Member of AIAA.

been limited due to the incomplete predictability of failure modes and lifetimes of structures made of these materials.[5] Although interest has resulted from their high strength-to-weight ratios and their ability to be "tailor-made" for a particular application, composite materials have material properties determined by the interactions of the often dissimilar components that compose them. Consequently, even though composites can have lighter weight, greater strength, and other desirable properties when compared to the materials that they replace, they are often difficult to characterize and monitor using conventional analytic and diagnostic techniques. These significant impediments to the increased use of composite materials could be removed if ways can be found to monitor structural response. This paper explores the potential of using embedded fiber optic sensors to partially achieve this goal.

2. Interferometric Fiber Optic Sensing

A number of fiber optic methods have been developed for the inspection of critical components of mechanical structures.[6] The majority of fiber optic sensors utilize one of two basic principles in their operation; (1) a change in amplitude (intensity) of the light, or (2) a change in phase of the light as the light propagates through an optical arrangement that contains fiber-optic sensing elements. The sensors described in this paper fall into the latter category and are classified as interferometric.

Interferometric fiber optic sensors have been used for the detection of dynamic and static strain.[7] In dynamic applications, hetrodyne detection is often applied, and the measurement of an alternating strain reduces to a measurement of phase modulation, or frequency modulation of the optical carrier frequency. Optical path length changes can also be measured using linear frequency modulation of the optical source. In this case, the measurement of the path length is reduced to a measurement of a change in the beat frequency of the system.

When measuring static strains, phase changes must be measured. One alternative is to generate strain-induced phase shifts, detectable through shifting interference fringes. This approach has been applied to optical fibers bonded on the surface of test specimens,[8,9] and forms the basis for the embedded sensing methods applied herein.

3. Analysis

As shown in Figure 1, light from a Krypton laser is introduced into the test and reference fibers using a bidirectional coupler. The test fiber is shown embedded in a portion of a composite specimen subjected to pure bending. The exit ends of both fibers are placed near each other so that the spherical waves emitted interfere to produce Young's fringes. As loads are applied to the specimen, the fringes move and the number of fringes that pass a fixed spatial location is proportional to the strain.

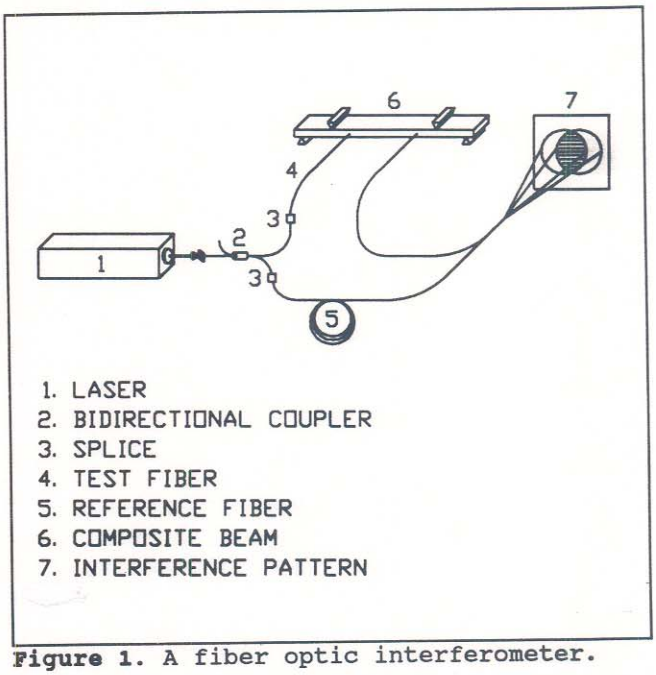

Figure 1. A fiber optic interferometer.

Following an argument presented by Sirkis and Taylor[10], the complex amplitude of the light emitted from the fibers can be expressed by

$$\Gamma_s = Ae^{i(\phi_s - \delta/2)} \quad (1)$$

$$\Gamma_r = Ae^{i(\phi_r + \delta/2)} \quad (2)$$

where $\delta/2$ is the relative phase change associated with each fiber. ϕ_s and ϕ_r are the phases associated with the waveform, expressed as

$$\phi_s = 2\pi/\lambda \, [(x_o - b/2)^2 + y_o^2 + z_o^2]^{1/2} \quad (3)$$

$$\phi_r = 2\pi/\lambda \, [(x_o + b/2)^2 + y_o^2 + z_o^2]^{1/2} \quad (4)$$

where the coordinates x_o, y_o, and z_o are defined on the source plane as shown in Figure 2, and b is the spacing between the two fibers.

The intensity of the light falling on a screen placed in front of the fibers is

$$I = A^2 + B^2 + 2AB \cos[-(2\pi/\lambda)(x_o b/z_o) + \delta]. \quad (5)$$

The intensity changes at a fixed point are introduced through the cosine term where the strain-induced phase shift δ results from the changes in the optical path length between the sensing and reference fibers. If a differential section of the fiber is isolated for an incremental strain, then the optical path length is given by

$$\Delta(nl) = l\Delta n + n\Delta l \quad (6)$$

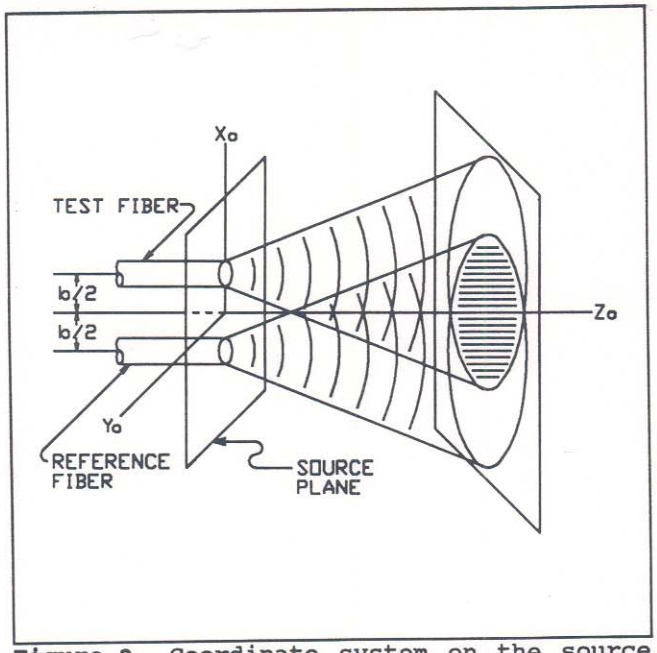

Figure 2. Coordinate system on the source plane.

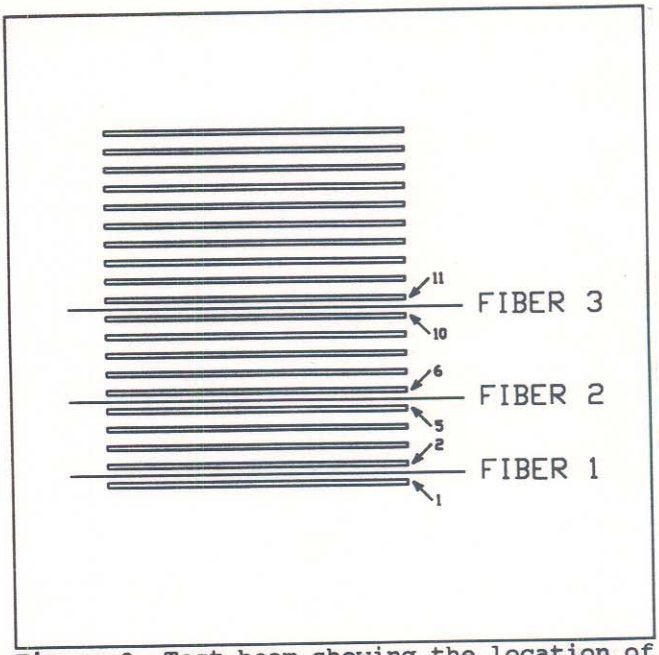

Figure 3. Test beam showing the location of embedded fibers.

where $l\Delta n$ is the component of the optical path length change due to change in refractive index and $n\Delta l$ is the component of change due to the change in fiber length.

In practice, the optical response of the interference fringes can be calibrated by subjecting a test specimen with an embedded fiber to a known strain. The incremental strain can then be expressed as

$$\epsilon = K \Delta k \qquad (7)$$

where Δk is the number of fringes passing over a photodetector positioned in the interference zone of the test and reference fibers.

4. Experimental

To demonstrate the method, twenty layers of pre-impregnated kevlar29/epoxy tape were hand laid to form a beam approximately 30.5 cm long, 2.54 cm wide, and 0.476 cm thick. The direction of maximum material strength of each lamina was oriented parallel to the longitudinal axis of the beam. As shown in Figure 3, optical fibers were embedded, during the lay-up, between layers 1 and 2, 5 and 6, and 10 and 11. These fibers are referred to as fibers 1, 2, and 3, respectively.

As illustrated in Figure 1 the composite beam was loaded to produce pure bending across 17.78 cm of the central span. Each fiber entered and exited the beam from one side so that a total fiber length of 12.70 cm was embedded. A 10.16 cm length test section of the fiber was placed in pure bending by running it parallel to the longitudinal axis of the beam. This geometry and loading were chosen so that stress concentrations near the load points did not significantly influence results, the fibers in the test section were in uniaxial tension, and the contribution to the phase difference by the remaining 2.54 cm of embedded fiber was minimized. Electrical resistance strain gages were mounted at the center of the span on the upper and lower surfaces of the beam.

The reference and object fibers were aligned to produce an interference pattern similar to that shown in Figure 4. The fringe shift, Δk, was observed, by eye, as strain was applied to the composite beam.

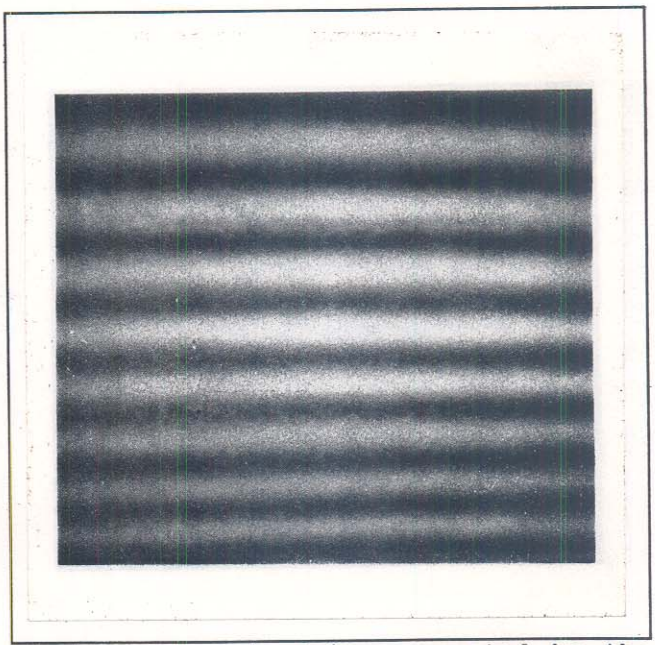

Figure 4. Young's fringes created by the interference of the object and reference fibers.

The fringe shift corresponds to the

line integral of the strain over the length of the fiber. A shift of one fringe corresponds to an angular phase change of 2π, or, a linear pathlength difference of λ/n; where λ is the wavelength and n is the index of refraction of the fiber.

Since the strain in the fiber is constant over the gage length, it is possible to establish a value for K in Equation (7). Strain can be computed by dividing the total linear pathlength difference, $\Delta k(\lambda/n)$, by the gage length, and

$$\epsilon = \Delta k\ \lambda/nl. \qquad (9)$$

Equating Equations (8) and (9),

$$K = \lambda/nl. \qquad (10)$$

For λ = 647.1 nm, n = 1.4571, and l = 10.16 cm, K = 4.371 $\mu\epsilon$/fringe.

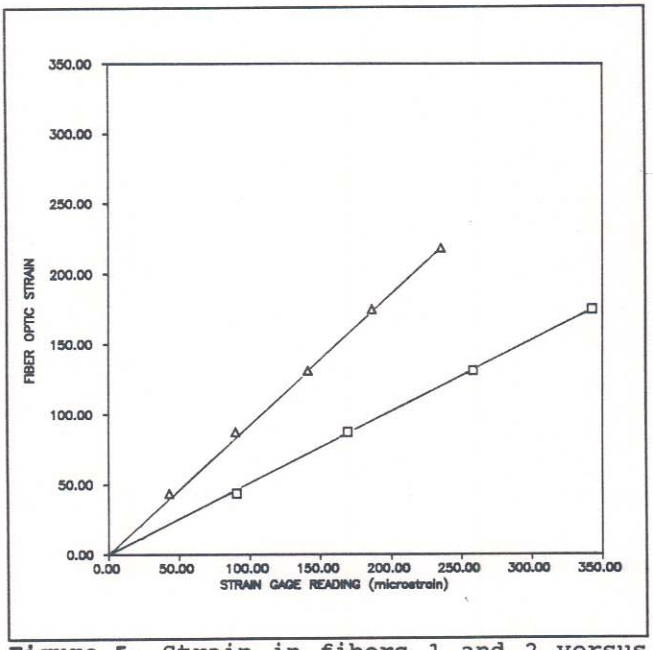

Figure 5. Strain in fibers 1 and 2 versus strain measured by the strain gages.

Figure 5 shows a plot of the strain in fibers 1 and 2 versus strain measured by the strain gages. Strains in the optical fibers were evaluated by counting fringe shifts and then applying Equation (7). No fringe shifts were observed for fiber 3, as would be expected, since fiber 3 lies along the neutral axis of the composite beam.

A direct correlation of the readings taken from the strain gages and the embedded fibers can be obtained by comparing the slopes of the plots in Figure 6 with the ratios obtained by dividing the distance that each fiber is located from the neutral axis by the distance from the neutral axis to the free surface. This comparison is valid, since strain varies linearly with distance from the neutral axis. The slopes for fibers 1 and 2 are 0.928 and 0.510, respectively, and the ratios of their relative positions are 0.9 and 0.5, respectively. These values agree to within three percent.

5. Discussion

The preceding discussions and results pertain to a relatively simple composite geometry under uniaxial stress. However, these restrictions are not as limited as they might appear, since engineering applications which involve these conditions include certain thin-walled pressure vessels and aircraft wings. For more complex composite structures and loading conditions, embedded sensing will be more difficult. For example, the direction of the composite fibers surrounding the optical fibers must be taken into consideration, and micro-mechanical effects of embedding optical fiber elements must be known. Once these factors are determined, and accurate coupling and fiber optic connection techniques as well as proper signal conditioning and interrogation methods are developed, the smart sensing approach considered herein will provide a valuable tool for aircraft diagnostics.

6. Conclusions

The results of this study show that embedded fiber optics can be used to accurately measure static strains in filament composites. The technology may ultimately provide the opportunity to understand the nature of the composite material including failure mechanisms and an assessment of remaining vehicle lifetime. There is also the potential for real time in-service monitoring of structural parameters including load determination, damage assessment, and structural dynamics (vibration) evaluation.

7. Acknowledgements

The authors would like to thank Nora Sassenfeld and Leigh Wilson for helping survey the literature. Portions of this research were supported under Contract No. NAG8-821 awarded to Dr. Gilbert by NASA's George C. Marshall Space Flight Center.

8. References

[1] Mazur, C.J., Sendeckyj, G.P., Stevens, D.M., "Air Force Smart Structures/Skins program overview," SPIE Vol. 986 Fiber Optic Smart Structures and Skins (1988), pp. 19-29.

[2] Claus, R.O., Safaai-Jazi, A., Bennett, K.D., May, R.G., Duncan, B.D., Vengsarkar, A.M., "Smart structures research program at Virginia Tech," SPIE Vol. 986 Fiber Optic Smart Structures and Skins (1988), pp 12-18.

[3] Jensen, D.W., Griffiths, R.W., "Optical fiber sensing considerations for a smart aerospace structure," SPIE Vol. 986 Fiber Optic Smart Structures and Skins (1988), pp. 70-76.

[4] Barrick, M.D., "Producibility and life cycle cost issues in applications of embedded fiber optic sensors in smart skins," SPIE Vol. 986 Fiber Optic Smart Structures and Skins (1988), pp. 171-179.

[5] Spillman, W.B., Jr., "Fiber optic sensors for composite monitoring," SPIE Vol. 986 Fiber Optic Smart Structures and Skins (1988), pp. 6-11.

[6] Bruinsma, S.J.A., "Review of fiber optic methods for strain monitoring and non-destructive testing," SPIE Vol. 1011 Fiber Optic Sensors III (1988), pp. 122-129.

[7] Uttam, D., Culshaw, B., Ward, J.D., Carter, D., "Interferometric optical fibre strain measurement," J. Phys. E: Sci. Instrum., Vol. 18, 1985, pp. 290-294.

[8] Butter, C.D., Hocker, G.B., "Fiber optics strain gauge," Applied Optics, Vol. 17, No. 18, 1978, pp. 2867-2869.

[9] Sirkis, J.S., Taylor, C.E., "Interferometric-fiber-optic strain sensor," Experimental Mechanics, Vol. 28, No. 2, 1988, pp. 170-176.

[10] Society for Experimental Mechanics, Inc., Handbook On Experimental Mechanics, Edited by Albert S. Kobayashi, Prentice-Hall, Inc., Englewood Cliffs, N.J., 1987; see Section 2-7, "Fiber-Optic Sensors," pp. 72-78.